Cloaking of Slot Antennas at C-Band Frequencies Using Elliptical Metasurface Cloaks

Shefali Pawar, *Student Member, IEEE*, Harry G. Skinner, *Member, IEEE*, Seong-Youp Suh, *Senior Member, IEEE*, and Alexander B. Yakovlev, *Senior Member, IEEE*

***Abstract*— In this letter, we endeavor to curb the adverse effects of mutual coupling between two-slot antennas (operating at C-band frequencies), situated at a subwavelength separation. The effects of mutual coupling become extremely apparent at such close proximity and leads to the deterioration of the radiation aspects of each antenna. To mitigate these detrimental effects, we exploit the concept of mantle cloaking for the design of specialized cloaks, consisting of elliptical dielectric regions integrated with capacitive metallic strips. It is demonstrated through simulation results that by enclosing each radiating edge of the individual slots with these uniquely designed metasurfaces, the slot antennas are decoupled in the near field. Moreover, the metasurface cloaks also facilitate restoration of the far field radiation properties of the slots. In this regard, our cloak design ensures that the slot antennas do not sense the presence of each other, enabling each slot antenna to operate individually, as if they were isolated.**

***Index Terms*—Elliptical metasurface, mantle cloaking, mutual coupling, radiation characteristics, slot antennas.**

I. Introduction

THE concept of invisibility has always been a subject of fascination to mankind and needless to say, it has become a trending topic for research in the academic circles. Consequently, a significant amount of research work is being dedicated toward the achievement of invisibility, specifically, electromagnetic invisibility. As such, over the past few decades, electromagnetic invisibility has emerged as an interesting application of metamaterials. One of the most commonly used techniques that can induce electromagnetic invisibility is transformation optics [1]–[3]. Although it is in principle a viable way to cloak the objects over a range of desired frequencies, it suffers from several limitations, such as narrow bandwidths, the usage of complex and precise inhomogeneity profiles, and dielectric/conduction losses in metamaterials. Other prominent methodologies include plasmonic cloaking [4]–[6] and transmission-line networks [7]–[8], which essentially overcomes the narrow bandwidth of other cloaking techniques. However, all of these techniques suffer from a prevalent drawback; they rely on bulk volumetric metamaterials with finite thickness, typically proportionate to the size of the object being cloaked. This leads to difficulties in the practical realization of these structures, especially in applications that require dense environments with many closely spaced objects. To rise up to this challenge, a cloaking method based on the concept of scattering cancellation, labeled mantle cloaking, was put forth to reduce the scattering width of different objects [9]–[13]. As a further extension, this technique has also been exploited for the cloaking of elliptical cylinders and two-dimensional (2-D) metallic strips [14]–[15]. The mantle cloaking method has also been implemented at low-terahertz (THz) frequencies, whereas a graphene monolayer and a nanostructured graphene patch array is used for planar and cylindrical objects [16]–[17].

It is known that antennas form the very core of the modern wireless communication systems and an escalating demand for increase in the wireless system capacity entails accommodation of densely packed antennas in a very compact space. However, a practical design of such a system is not only cumbersome but it also leads to the deterioration of the overall system performance, on account of the mutual interaction between the closely spaced antennas. The mantle cloaking method has been proven useful in overcoming this issue presented in [18] and [19]. The mantle cloaking of elliptical cylinders, in particular 2-D metallic strips, influenced the extension of this concept to freestanding strip dipole antennas [20] and planar microstrip monopoles [21]–[22]. These explicitly designed metasurface cloaks are known to produce a cloaking effect in such a way that the neighboring antennas do not sense the presence of each other [23], [24]. Similarly, graphene-based metasurfaces are used to overcome the interference due to mutual coupling between strip dipole antennas [25] and planar antennas [26], at low-THz frequencies. In [27], wideband cloaking of microstrip monopoles is achieved, and in [28], graphene-based wideband tunable scattering cancellation (terahertz spectrum) is realized by applying mantle cloaking approach. Very recently, the concept of decoupling and cloaking using mantle cloaks has also been applied to interleaved phased arrays of free standing strip monopole antennas [29] and printed monopole antennas at microwave frequencies [30]–[31]. The idea is further protracted to cloaking of one-dimensional (1-D) and 2-D of microstrip dipole arrays [32].

In this letter, we have applied the concept of mantle cloaking, in order to facilitate the efficient performance of the two slot antennas, in spite of them being situated very close to

Manuscript received 26 May 2022; accepted 11 July 2022. Date of publication 22 July 2022; date of current version 28 October 2022. This work was supported in part by the NSF I/UCRC under Grant 1822104 and in part by the Intel Corporation. *(Corresponding author: Shefali Pawar.)*

Shefali Pawar and Alexander B. Yakovlev are with the Department of Electrical Engineering, University of Mississippi, University, MS 38677 USA (e-mail: pawarshefali198@gmail.com; yakovlev@olemiss.edu).

Harry G. Skinner and Seong-Youp Suh are with Intel Corporation, Hillsboro, OR 97124 USA (e-mail: harry.g.skinner@intel.com; seong-youp.suh@intel.com).

Digital Object Identifier 10.1109/LAWP.2022.3193038

each other. Accordingly, we have considered two slot antennas, namely Slot I and Slot II, designed to operate at gigahertz (GHz) frequencies (specifically focusing on the C-band frequencies for fifth-generation (5G) wireless applications). The novelty of our cloak structure lies in the use of elliptical dielectrics incorporated with two perfect electric conductor (PEC) strips, acting as capacitive strips, on its surface, such that when they are wrapped around each radiating edge of the individual slot antennas, the metasurface cloaks not only restore their radiation patterns, but also act as a filter, essentially making Slot I a poor radiator at the resonance frequency of Slot II and vice versa. It is also established that the far field patterns of the slots are restored as if they were two isolated antennas. The design procedure and all the numerical full-wave simulations presented in this letter are obtained with the CST Microwave Studio [33].

II. Decoupling and Cloaking of Slot Antennas

Our assessment begins with the schematic design of two slot antennas (essentially slots cut in a rectangular metallic sheet). These slot antennas, designated as Slots I and II, are intended to operate at frequencies $f_1 =$ 4.5 GHz and $f_2 =$ 5.5 GHz, respectively. All the variables used to denote geometrical dimensions in this letter are measured in millimeters (mm). Fig. 1(a) and (b) shows the uncloaked and cloaked structures for the slot antennas, respectively, whereas Fig. 1(c) shows a side view of the cloaked antennas, to give a detailed insight into the construct of the metasurface cloaks. The list of parameters shown in Fig. 1 are: $L = 180$, $W = 180$, $L_1 = 34.8$, $W_1 = W_2 = 1.5$, $L_2 = 28.5$, $W_{s1} = 0.97$, $D_1 = 1.17$, $W_{s2} = 0.843$, $D_2 = 1.143$, $a_1 = a_2 = 0.5$, $b_1 = 0.218$, $b_2 = 0.196$, $\varepsilon_{c1} = 4.5$, and $\varepsilon_{c2} = 2.1$. First, we analyze each individual slot antennas in the isolated scenario (i.e., each antenna is analyzed in the absence of the other antenna); we label this scenario as the *isolated case*. We then proceed with our analysis by placing the uncloaked slots very close to each other (at a subwavelength span of $g = 3$ mm, which is 0.045 λ_1 or 0.055 λ_2 approximately; λ_1 and λ_2 are the wavelengths corresponding to the frequencies f_1 and f_2, respectively); this scenario is called as the *uncloaked coupled case*. As expected, the close proximity of the antennas generates a mutual interference in the near field as well as the far field, which deteriorates the matching and radiation characteristics of both the antennas. In order to minimize the adverse effects of mutual coupling, the corresponding elliptical metasurface cloaks are enclosed around each radiating edge of the slots; this scenario is aptly named as the *cloaked decoupled case*. We initiated the design process for our proposed metasurface cloak [see Fig. 1(b)] by modeling cloaking structures for the isolated Slots I and II and then placed these cloaked slots in close proximity to observe the desired decoupling and cloaking effect. In our cloak design, for each of the slots, two PEC strips are symmetrically arranged along the curved surface of each elliptical dielectric, such that one strip passes through the hollow region of the respective slot while the other passes through the metallic sheet, with two gaps in between the strips [see Fig. 1(c)]. The width of the PEC strips is larger than the gap between the two strips, making the cloaks appear like a

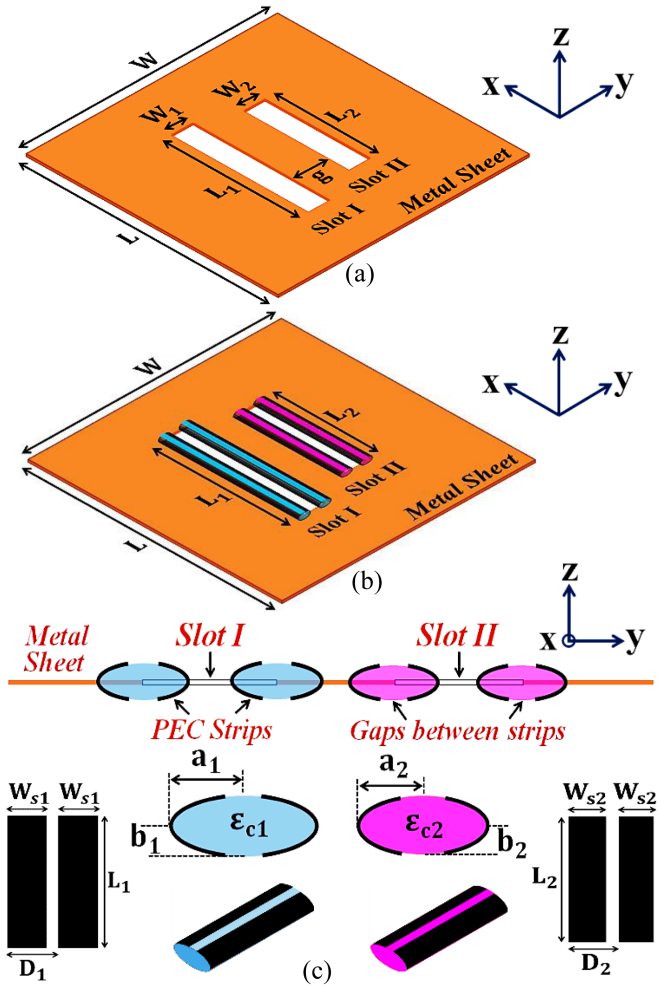

Fig. 1. (a) Uncloaked, (b) cloaked schematics of Slots I and II, and (c) side view of the cloaked slot antennas.

slotted structure. Now consider the cloak structure for each individual slot, e.g., Slot I. Through multiple experimentations, we established that it is imperative for one of the PEC strips on each dielectric surface to maintain contact with the metal sheet.

It is our understanding that this particular arrangement of the PEC strips leads to the redistribution of charges from the edges of the slot (in the uncloaked case) to the surface of the metallic part of the elliptical metasurface, compelling the metasurface to resemble an equipotential surface. This peculiar behavior leads to an apparent shielding effect, which in turn leads to concentration of the electric field (E-field) in between the arcs of the PEC strips within the slot [see Fig. 2(b) and (c)].

However, this phenomenon does not affect the efficiency or the gain of the slot antenna at its resonance frequency (in this case, 4.5 GHz). In fact, the only apparent effect is the narrower bandwidth of the cloaked Slot I [see Fig. 2(a)] as the effective width of the slot is reduced. Similar arguments can be made for Slot II. The role of the gap between the strips is critical, as the neighboring slot excites its cloak, inducing E-fields on these gaps (as equivalent magnetic surface currents). In our view, these induced fields are responsible for the cancellation of the scattered fields emanating from the slot, leading to the suppression of the fields within the slot, which in turn curbs

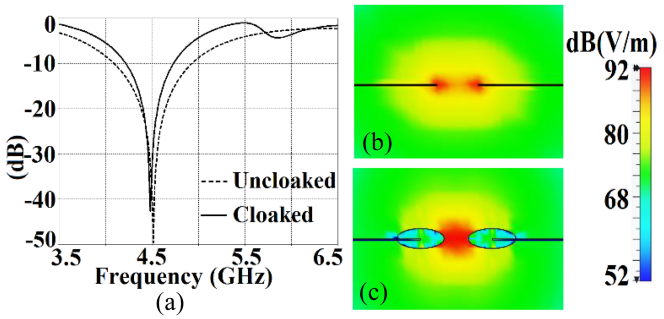

Fig. 2. (a) *S*-parameter plot and E-field distributions for (b) isolated uncloaked and (c) isolated cloaked Slot I.

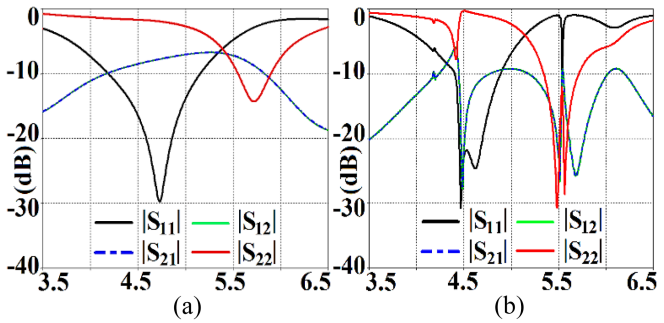

Fig. 3. *S*-parameter plots for (a) uncloaked coupled and (b) cloaked decoupled slot antennas.

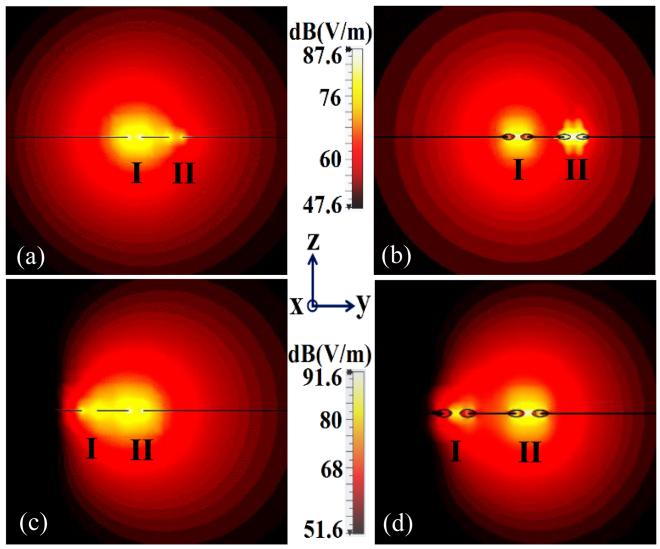

Fig. 4. E-field distributions for (a) uncloaked coupled and (b) cloaked decoupled when Slot I is active, and (c) uncloaked coupled and (d) cloaked decoupled when Slot II is active.

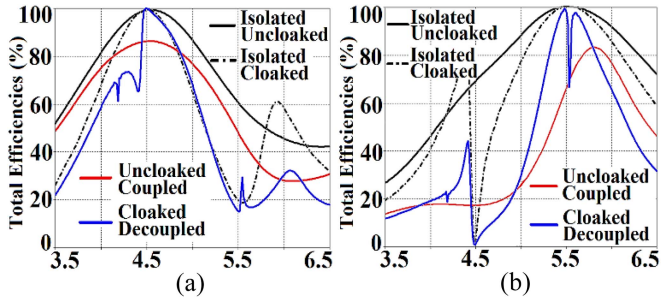

Fig. 5. Plots for total efficiencies. (a) Slot I ($f_1 = 4.5$ GHz) is active. (b) Slot II ($f_2 = 5.5$ GHz) is active.

the near-field as well as far-field interaction between the two slots. Thus, the uniquely designed metasurfaces are successful in achieving decoupling of the slot antennas in the near field as well as cloaking in the far field. The optimum values for the width of the PEC strips and the permittivity of the dielectric regions was found by conducting extensive parametric analysis. We also observed that the E-field of the cloaked slots, in the presence of the elliptically shaped metasurface, emulates the natural E-field of the uncloaked slots and that the parameters of the cloaks are much easier to control as compared with the circular metasurfaces; hence, an ellipse is preferred. The S-parameter plots (see Fig. 3) prove the decoupling effect of the elliptical metasurface cloaks, and the snapshots of the E-field distributions (see Fig. 4) further validate this claim.

It is clearly seen from Fig. 3(a) that the coupling coefficients $|S_{12}| = |S_{21}| > -10$ dB (uncloaked coupled case) at both f_1 and f_2, indicating strong mutual coupling between Slots I and II. On the other hand, in Fig. 3(b) (cloaked decoupled case), a substantial decrement in $|S_{12}|$ and $|S_{21}|$ can be seen; a reduction of almost 20 dB at both f_1 and f_2 is noted. From Fig. 3(b), we can also observe that $|S_{22}| = 0$ dB at the resonance frequency f_1, indicating that Slot II is completely decoupled at f_1. Similarly, $|S_{11}| \approx 0$ dB, at the resonance frequency f_2, indicating that Slot I is decoupled at f_2. The cross-sectional view of the E-field contours is presented for the uncloaked and cloaked slot antennas in Fig. 4(a) and (b), respectively, wherein Slot I ($f_1 = 4.5$ GHz) is excited, keeping Slot II ($f_2 = 5.5$ GHz) inactive. The presence of mutual coupling is demonstrated for the uncloaked case [see Fig. 4(a), where a high concentration of E-field in the area between the two slots is visible, shown by the yellow colored region], essentially enabling the power to be coupled from Slot I to the port of the neighboring slot (Slot II).

However, when the metasurfaces are employed, they evidently reduce the E-field interaction between the slots [cloaked case, see Fig. 4(b), where the cloaks seem to confine the E-fields, leading to the reduction of field concentration in the area between the slots], ostensibly making the radiating parts of the slot antennas invisible to each other. Similar observations can be made from Fig. 4(c) and (d), where Slot II is active and Slot I is kept passive. Thus, we can conclude that when the slots are cloaked, the electric field produced by one slot is not sensed by the input port of the neighboring slot, illustrating the decoupling effect of the metasurface cloaks. We further present the comparison of the total efficiencies of the slot antennas for isolated, uncloaked, and cloaked conditions in Fig. 5. The total efficiency is calculated as: $\eta_{\text{total}} = (1 - |\Gamma|^2)\eta$, where η_{total} is the total efficiency, Γ is the reflection coefficient (S_{11} or S_{22}), and η is the radiation efficiency for the respective slot antennas. The mutual coupling between the uncloaked antennas causes a drop of almost 13% and a reduction of almost 19% in the total efficiency of Slots I

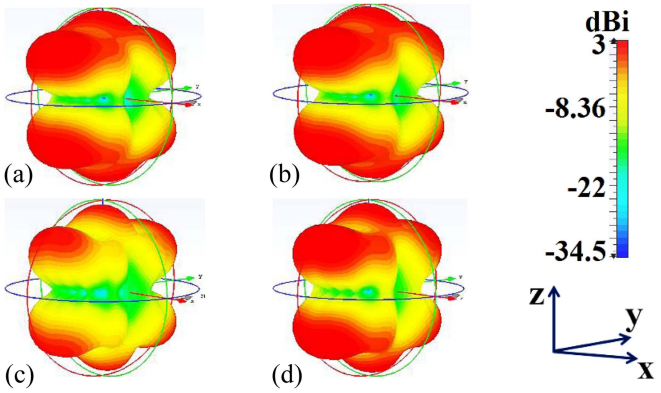

Fig. 6. 3-D radiation patterns for Slot I ($f_1 = 4.5$ GHz). (a) Isolated uncloaked. (b) Isolated cloaked. (c) Uncloaked coupled. (d) Cloaked decoupled.

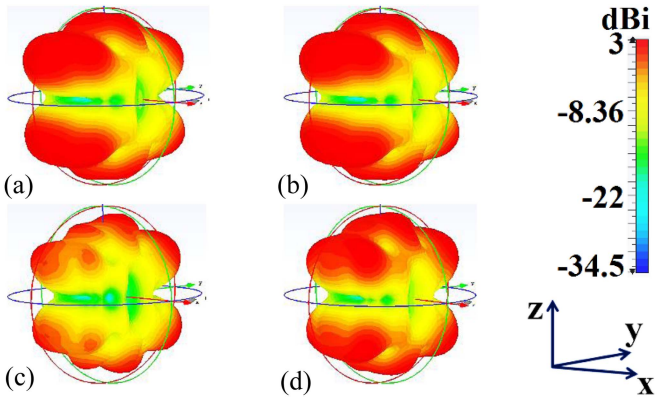

Fig. 7. 3-D radiation patterns for Slot II ($f_2 = 5.5$ GHz). (a) Isolated uncloaked. (b) Isolated cloaked. (c) Uncloaked coupled. (d) Cloaked decoupled.

and II, respectively [shown by the red curves in Fig. 5(a) and (b)].

The drop in the total efficiencies for the uncloaked antennas is improved for the cloaked case (shown by the blue curves in Fig. 5), and the efficiencies are equivalent to that of the isolated cases. An important trait of our metasurface cloak design is that it does not perturb the radiation characteristics of the antenna which it envelops; rather its effect manifests at the frequency of the other antenna in its vicinity. This is ascertained from the plots in Fig. 5(a), where it can be seen that the total efficiency of Slot I remains unaffected at its own frequency ($f_1 = 4.5$ GHz), but is reduced almost to 17% at the resonance frequency of Slot II ($f_2 = 5.5$ GHz). Similarly, from Fig. 5(b), we note that the total efficiency of Slot II stays at full efficiency at its frequency ($f_2 = 5.5$ GHz), but is reduced to zero at the resonance frequency of Slot I ($f_1 = 4.5$ GHz). Simply put the metasurface around Slot I compels itself to become a poor radiator, while also making its scattering residual at the resonance frequency of Slot II and vice versa. The simulated three-dimensional (3-D) radiation patterns for Slot I (see Fig. 6) and Slot II (see Fig. 7) as well as their polar plots (see Fig. 8), all confirm the aforementioned claim. It follows that the presence of the cloaks leads to the suppression of the far-field coupling as well.

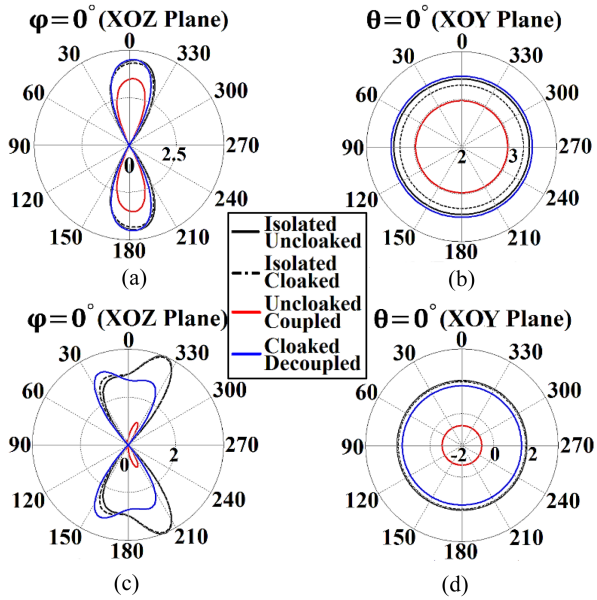

Fig. 8. Polar plots at (a) $\varphi = 0^\circ$ and (b) $\theta = 0^\circ$ for Slot I ($f_1 = 4.5$ GHz), and at (c) $\varphi = 0^\circ$ and (d) $\theta = 0^\circ$ for Slot II ($f_2 = 5.5$ GHz). (a) and (c) θ (degrees). (b) and (d) φ (degrees).

The realized gain of each antenna is around 4.2 dBi in the isolated scenario. However, when the antennas are placed close to each other (uncloaked coupled case), it leads to the distortion in the radiation patterns for Slots I and II, which is apparent from Figs. 6(c) and 7(c), respectively. Furthermore, it can be deduced from Figs. 6(d) and7(d) (cloaked decoupled case) that the elliptical cloaks successfully restore the radiation patterns of the slot antennas. Moreover, the restored patterns resemble the radiation patterns of the antennas in the isolated scenario. Note that the 3-D patterns for isolated uncloaked and isolated cloaked cases are practically identical [see Fig. 6(a) and (b) for Slot I, and Fig. 7(a) and (b) for Slot II], thereby exemplifying that the elliptical cloaks do not affect the properties of the antenna elements they are designed for. We finally present the polar plots in Fig. 8 for the realized gain of each slot antenna, at $\varphi = 0^\circ$ and $\theta = 0^\circ$ reference planes. For the uncloaked coupled case, a decrease of 1.33 dBi in the main lobe gain is recorded at both the planes for Slot I [see Fig. 8(a) and (b)], whereas a decrement of almost 3 dBi is seen at both the planes for Slot II [see Fig. 8(c) and (d)]. For the cloaked decoupled case, it is apparent that the engineered cloaks faithfully rehabilitate the realized gain for both the slots, at both planes of reference.

III. Conclusion

We propose a novel cloak structure in order to decouple two slot antennas, placed at a subwavelength separation, with the intention to recover their matching properties and restore their radiation characteristics. Accordingly, the explicit elliptical metasurfaces ensure that the slots are decoupled and their radiation patterns are reinstated in such a way that it emulates an isolated operation of each slot antenna. Hence, we have put forth a design that can lead to densely packed slot antenna systems with vastly improved performance and high efficiency.

REFERENCES

[1] J. Pendry, D. Schurig, and D. Smith, "Controlling electromagnetic fields," *Science*, vol. 312, no. 5781, pp. 1780–1782, Jun. 2006, doi: 10.1126/science.1125907.

[2] H. Chen, C. Chan, and P. Sheng, "Transformation optics and metamaterials," *Nature Mater.*, vol. 9, no. 5, pp. 387–396, May 2010, doi: 10.1038/nmat2743.

[3] A. Vakil and N. Engheta, "Transformation optics using graphene," *Science*, vol. 332, no. 6035, pp. 1291–1294, Jun. 2011, doi: 10.1126/science.1202691.

[4] A. Alù and N. Engheta, "Achieving transparency with plasmonic and metamaterial coatings," *Phys. Rev. E*, vol. 72, Jul. 2005, Art. no. 016623, doi: 10.1103/PhysRevE.72.016623.

[5] A. Alù and N. Engheta, "Cloaking and transparency for collections of particles with metamaterial and plasmonic covers," *Opt. Exp.*, vol. 15, no. 12, pp. 7578–7590, Jun. 2007, doi: 10.1364/OE.15.007578.

[6] B. Edwards, A. Alù, M. Silveirinha, and N. Engheta, "Experimental verification of plasmonic cloaking at microwave frequencies with metamaterials," *Phys. Rev. Lett.*, vol. 103, no. 15, Oct. 2009, Art. no. 153901, doi: 10.1103/PHYSREVLETT.103.153901.

[7] P. Alitalo, O. Luukkonen, L. Jylha, J. Venermo, and S. Tretyakov, "Transmission-line networks cloaking objects from electromagnetic fields," *IEEE Trans. Antennas Propag.*, vol. 56, no. 2, pp. 416–424, Feb. 2008, doi: 10.1109/TAP.2007.915469.

[8] P. Alitalo, J. Vehmas, and S. Tretyakov, "Reduction of antenna blockage with a transmission-line cloak," in *Proc. Eur. Conf. Antennas Propag.*, 2011, pp. 2399–2402.

[9] A. Alù, "Mantle cloak: Invisibility induced by a surface," *Phys. Rev. B*, vol. 80, no. 24, Dec. 2009, Art. no. 245115, doi: 10.1103/PhysRevB.80.245115.

[10] P. Chen and A. Alù, "Mantle cloaking using thin patterned metasurfaces," *Phys. Rev. B*, vol. 84, no. 20, Nov. 2011, Art. no. 205110, doi: 10.1103/PhysRevB.84.205110.

[11] Y. Padooru, A. Yakovlev, P. Chen, and A. Alù, "Analytical modeling of conformal mantle cloaks for cylindrical objects using sub-wavelength printed and slotted arrays," *J. Appl. Phys.*, vol. 112, no. 3, Aug. 2012, Art. no. 034907, doi: 10.1063/1.4745888.

[12] L. Matekovits and T. Bird, "Width-modulated microstrip-line based mantle cloaks for thin single and multiple cylinders," *IEEE Trans. Antennas Propag.*, vol. 62, no. 5, pp. 2606–2615, May 2014, doi: 10.1109/TAP.2014.2307587.

[13] Z. Hamzavi-Zarghani, A. Yahaghi, and L. Matekovits, "Analytical design of a metasurface based mantle cloak for dielectric cylinder under oblique incidence," in *Proc. Int. Symp. Telecommun.*, 2018, pp. 65–68.

[14] H. Bernety and A. Yakovlev, "Conformal and confocal mantle cloaking of elliptical cylinders using sub-wavelength metallic meshes and patches," in *Proc. IEEE Antennas Propag. Soc. Int. Symp.*, 2014, pp. 1433–1434.

[15] H. Bernety and A. Yakovlev, "Cloaking of single and multiple elliptical cylinders and strips with confocal elliptical nanostructured graphene metasurface," *J. Phys. Condens. Matter*, vol. 27, no. 18, Apr. 2015, Art. no. 185304.

[16] P. Chen and A. Alù, "Atomically-thin surface cloak using graphene monolayers," *ACS Nano*, vol. 5, no. 7, pp. 5855–5863, Jun. 2011, doi: 10.1021/nn201622e.

[17] P. Chen, J. Soric, Y. Padooru, H. Bernety, A. Yakovlev, and A. Alù, "Nanostructured graphene metasurface for tunable terahertz cloaking," *New J. Phys.*, vol. 15, Dec. 2013, Art. no. 123029.

[18] A. Monti, J. Soric, A. Alù, F. Bilotti, A. Toscano, and L. Vegni, "Overcoming mutual blockage between neighboring dipole antennas using a low-profile patterned metasurface," *IEEE Antennas Wireless Propag. Lett.*, vol. 11, pp. 1414–1417, 2012, doi: 10.1109/LAWP.2012.2229102.

[19] J. Soric, A. Monti, A. Toscano, F. Bilotti, and A. Alù, "Dual-polarized reduction of dipole antenna blockage using mantle cloaks," *IEEE Trans. Antennas Propag.*, vol. 63, no. 11, pp. 4827–4834, Nov. 2015, doi: 10.1109/TAP.2015.2476468.

[20] H. Bernety and A. Yakovlev, "Reduction of mutual coupling between neighboring strip dipole antennas using confocal elliptical metasurface cloaks," *IEEE Trans. Antennas Propag.*, vol. 63, no. 4, pp. 1554–1563, Apr. 2015, doi: 10.1109/TAP.2015.2398121.

[21] H. Bernety and A. Yakovlev, "Decoupling antennas in printed technology using elliptical metasurface cloaks," *J. Appl. Phys.*, vol. 119, no. 1, Jan. 2016, Art. no. 014904, doi: 10.1063/1.4939610.

[22] S. Pawar et al., "Elliptical metasurface cloaks for decoupling and cloaking of microstrip monopole antennas at 28 GHz and 39 GHz for 5G wireless applications," in *Proc. IEEE Int. Symp. Antennas Propag. North Amer. Radio Sci. Meeting*, 2020, pp. 805–806.

[23] Z. Jiang and D. Werner, "Dispersion engineering of metasurfaces for dual-frequency quasi-three-dimensional cloaking of microwave radiators," *Opt. Exp.*, vol. 24, no. 9, pp. 9629–9644, Apr. 2016, doi: 10.1364/OE.24.009629.

[24] A. Monti et al., "Mantle cloaking for co-site radio-frequency antennas," *Appl. Phys. Lett.*, vol. 108, no. 11, Mar. 2016, Art. no. 113502, doi: 10.1063/1.4944042.

[25] G. Moreno, H.Mehrpour Bernety, and A. Yakovlev, "Reduction of mutual coupling between strip dipole antennas at terahertz frequencies with an elliptically shaped graphene monolayer," *IEEE Antenna Wireless Propag., Lett,* vol. 15, pp. 1533–1536, 2015, doi: 10.1109/LAWP.2015.2505333.

[26] J. Ghosh and D. Mitra, "Mutual coupling reduction in planar antenna by graphene metasurface for THz application," *J. Electromagn. Waves Appl.*, vol. 31, no. 18, pp. 2036–2045, Jan. 2017, doi: 10.1080/09205071.2016.1277959.

[27] G. Moreno et al., "Wideband elliptical metasurface cloaks in printed antenna technology," *IEEE Trans. Antennas Propag.*, vol. 66, no. 7, pp. 3512–3525, Jul. 2018, doi: 10.1109/TAP.2018.2829809.

[28] E. Shokati and N. Granpayeh, "Wideband cloaking by using inhomogeneous nanostructured graphene metasurface for tunable cloaking in the terahertz regime," in *Proc. Int. Conf. Millimeter-Wave Terahertz Technol.*, 2016, pp. 9–13.

[29] H. Mehrpour Bernety, A. Yakovlev, H. Skinner, S. Suh, and A. Alù, "Decoupling and cloaking of interleaved phased antenna arrays using elliptical metasurfaces," *IEEE Trans. Antennas Propag.*, vol. 68, no. 6, pp. 4997–5002, Jun. 2020, doi: 10.1109/TAP.2019.2957286.

[30] S. Pawar et al., "Cloaking and decoupling of interleaved microstrip monopole arrays at 28 GHz and 39 GHz using elliptical metasurfaces for 5G wireless applications," in *Proc. IEEE Int. Symp. Antennas Propag. North Amer. Radio Sci. Meeting*, 2020, pp. 869–870.

[31] S. Pawar, H. Mehrpour Bernety, H. G. Skinner, S.-Y. Suh, A. Alù, and A. B. Yakovlev, "Mantle cloaking for decoupling of interleaved phased antenna arrays in 5G applications," *AIP Conf. Proc.*, vol. 2300, no. 1, Dec. 2020, Art. no. 020095, doi: 10.1063/5.0031836.

[32] D. Lee and A. B. Yakovlev, "Metasurface cloaks to decouple closely spaced printed dipole antenna arrays fed by a microstrip-to-balanced transmission-line transition," *IEEE Access*, vol. 9, pp. 128209–128219, 2021, doi: 10.1109/ACCESS.2021.3112771.

[33] CST Microwave Studio, 2019. Jul. 30, 2022. [Online]. Available: https://www.cst.com